Ca^{2+}-Inositol Phosphate Chelation Mediates the Substrate Specificity of β-Propeller Phytase†

Byung-Chul Oh,*,‡ Myung Hee Kim,§ Bong-Sik Yun,§ Won-Chan Choi,§ Sung-Chun Park,|| Suk-Chul Bae,‡ and Tae-Kwang Oh*,§

Department of Biochemistry, School of Medicine, Chungbuk National University, Cheongju 361-763, South Korea, Microbial Genomics & Applications Center, Korea Research Institute of Bioscience and Biotechnology, Yusong, Daejeon 305-333, South Korea, and Comparative Pharmacokinetics & Microbial Pharmacology, College of Veterinary Medicine, Kyungpook National University, Daegu 702-701, South Korea

Received February 14, 2006; Revised Manuscript Received May 25, 2006

ABSTRACT: Inositol phosphates are recognized as having diverse and critical roles in biological systems. In this report, kinetic studies and TLC analysis indicate that β-propeller phytase is a special class of inositol phosphatase that preferentially recognizes a bidentate (P-Ca^{2+}-P) formed between Ca^{2+} and two adjacent phosphate groups of its natural substrate phytate ($InsP_6$). The specific recognition of a bidentate chelation enables the enzyme to sequentially hydrolyze one of the phosphate groups in a bidentate of $Ca^{2+}-InsP_6$ to yield a *myo*-inositol trisphosphate ($InsP_3$) and three phosphates as the final products. A comparative analysis of ^1H- and ^{13}C NMR spectroscopy with the aid of 2D NMR confirms that the chemical structure of the final product is *myo*-Ins(2,4,6)P_3. The catalytic properties of the enzyme suggest a potential model for how the enzyme specifically recognizes its substrate $Ca^{2+}-InsP_6$ and produces *myo*-Ins(2,4,6)-P_3 from $Ca^{2+}-InsP_6$. These findings potentially provide evidence for a selective $Ca^{2+}-$InsPs chelation between Ca^{2+} and two adjacent phosphate groups of inositol phosphates.

Chelation by phosphate involves the coordinate binding of the ligand to a metal ion by the donation of electrons from the oxygen atoms of the phosphate. Divalent cations such as Ca^{2+} and Mg^{2+}, which are the most abundant cations in biological systems (*1*, *2*), are more susceptible to chelation than monovalent ions. Thus, all naturally existing compounds with phosphate groups, such as cyclic phosphates, carbohydrate phosphates, and nucleotides, are potential chelators of Ca^{2+} and Mg^{2+}. With a single available phosphate group, these interactions are very weak, but they become stronger when two phosphate groups are close together. Moreover, the binding properties of phosphate groups depend on the ionic radius of the divalent cation as well as the number of phosphate groups (*3*). Of particular interest is the family of *myo*-inositol phosphates (InsPs[1]) because InsPs provide very favorable environments with multiple phosphate groups (*4*). For example, a single phosphate group on an inositol ring ($InsP_1$) or two long-distance phosphate groups, such as Ins-(1,4)P_2, prefer Mg^{2+} with its small ionic radius and form a monodentate chelation, whereas Ins(4,5)P_2 with two adjacent phosphate groups directly binds Ca^{2+} with its larger ionic radius. The latter is believed to form a bidentate (P-Ca^{2+}-P) chelation between Ca^{2+} and the two oxianions from the adjacent phosphate groups (Scheme 1) (*5*, *6*). Other biologically important compounds, such as Ins(1,4,5)P_3, Ins(1,3,4,5)-P_4, and phytate ($InsP_6$), also bind Ca^{2+} with high affinity over the physiological Ca^{2+} concentration range of $10^{-7}-10^{-3}$ M (*7*−*9*). In particular, $InsP_6$ is a strong chelator of Ca^{2+} and forms multiple bidentate chelations with Ca^{2+}. Therefore, $InsP_6$ inhibits the intestinal absorption of dietary Ca^{2+} (*6*) and cardiovascular calcifications (*10*−*12*) through strong Ca^{2+} chelation in biological systems.

Phytases are a class of inositol phosphatases that are responsible for the hydrolysis of $InsP_6$. These enzymes can be classified as histidine acid phytases (HAPs) and alkaline phytases on the basis of their pH optima (*13*−*17*). Several HAPs have been cloned and extensively characterized, including fungal phytases from *Aspergillus*, bacterial phytases (pH 2.5 acid phosphatase and glucose-1-phosphatase) from *Escherichia coli*, and mammalian phytases (rat hepatic multiple inositol phosphatase, human prostatic, and lysosomal acid phosphatases). These enzymes exhibit no apparent sequence similarity to each other or to other known phosphatases, except for a conserved RHGXRXP motif in their active sites that is essential for catalytic activity (*18*). Despite a lack of sequence similarity beyond the active site, the crystal structures closely resemble the overall fold of a large α/β and a smaller α-domain (*19*). Most known HAPs can be classified into one of two classes on the basis of substrate specificity. One class of HAPs exhibits a lower specific activity with broad specificity for a variety of phosphate-

† These studies were supported by the 21C Frontier R&D Program and the Creative Research Program (M10301000012, S-C Bae) from the Ministry of Science and Technology of Korea.

* To whom correspondence should be addressed. Phone: 82-43-261-3457. Fax: 82-43-274-8705. E-mail: bcoh@chungbuk.ac.kr (B.-C.O.); otk@kribb.re.kr (T.-K.O.).

‡ Chungbuk National University.

§ Korea Research Institute of Bioscience and Biotechnology.

|| Kyungpook National University.

[1] Abbreviations: HAPs, histidine acid phytases; InsPs, *myo*-inositol phosphates; IP3R, Ins(1,4,5)P_3 receptor; Phytate ($InsP_6$), *myo*-inositol1,2,3,4,5,6-hexakisphosphate; PtdInsPs, phosphatidyl inositol phosphates.

10.1021/bi0603118 CCC: $33.50
Published on Web 07/15/2006

Scheme 1: The Interaction between Inositol Phosphates and Divalent Cations

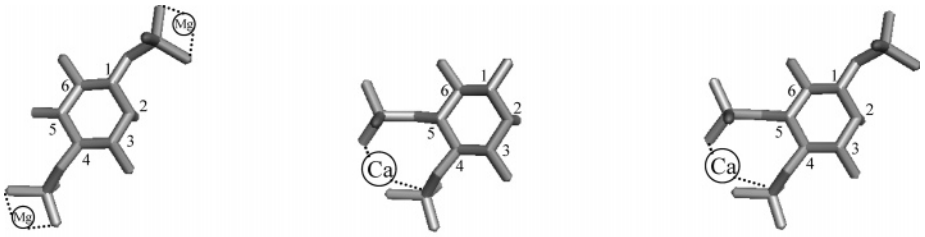

containing substrates, such as phenyl-phosphate, glucose-1-phosphate, glucose-6-phosphate, fructose-1-phosphate, and $InsP_6$. The other class of HAPs shows narrow substrate specificity with higher specific activity for $InsP_6$ (*20*). These HAPs can initially hydrolyze at the 3 or 6 position of $InsP_6$ to produce Ins2P as a final product (*13, 15, 16*).

Unlike HAPs, the phytases from *Bacillus* sp., *Shewanella oneidensis*, and plants differ in terms of substrate specificity, final products, and, perhaps most significantly, in the fact that Ca^{2+} is required for both enzyme activation and substrate recognition (*21*−*30*). These phytases form a special class of inositol phosphatases that lack the active site motif RHGXRXP found in HAPs and preferentially hydrolyze Ca^{2+}−$InsP_6$ to produce an $InsP_3$ as a final product (*21, 22, 25, 30*−*34*). We previously found that the crystal structure of alkaline phytase from *Bacillus* has two phosphate-group binding sites composed of a six-bladed β-propeller folding architecture (*35, 36*). This particular folding is designated as the active site for substrate phosphate group binding and is composed primarily of negatively charged amino acid groups, which provide a favorable electrostatic environment for Ca^{2+}−InsPs (*35*).

Despite the intense interest in InsPs and progress in characterizing inositol phosphatases, little is known about the kinetic mechanisms for substrate specificity determinants in this system. In this study, we have taken multiple approaches to better understand how β-propeller phytase preferentially recognizes its substrate Ca^{2+}−$InsP_6$ and how the enzyme selectively hydrolyzes Ca^{2+}−$InsP_6$ to yield *myo*-inositol 2,4,6-trisphosphate as a final product. The kinetic and NMR studies show that the chemical structure of the final product is *myo*-inositol 2,4,6-trisphosphate, which results from the specific binding properties of Ca^{2+} and $InsP_6$.

EXPERIMENTAL PROCEDURES

Protein Preparation. The gene encoding β-propeller phytase (amino acid residues 31−383) from *Bacillus amyloliquefaciens* DS11 was cloned into the vector pET22b (Novagen) and expressed with a 6× histidine tag in *E. coli* BL21 (DE3) (Novagen). The cells were initially grown in 50 mL of LB-ampicillin (100 μg/mL) for 8 h at 37 °C. Inocula were added to 2 L of LB-ampicillin (100 μg/mL). The large cultures were immediately moved to an incubator at 30 °C. When the cultures reached an A_{600} of 0.6−1.0, isopropyl-β-D-thiogalactopyranoside (IPTG) was added at a final concentration of 1 mM to induce the 6× His-tagged β-propeller phytase. After 3−4 h, the cells were harvested and lysed by sonication in an equilibrium buffer (50 mM Tris-HCl at pH 7.5, 250 mM NaCl, and 10 mM imidazole). Cell debris was removed by consecutive centrifugations at 4500*g* for 10 min and at 10 000*g* for 10 min at 4 °C. The soluble fraction was loaded onto a HR 10/10 column (Pharmacia) packed with 8 mL of nickel-nitrilotriacetic acid (Ni-NTA) superflow resin (Qiagen). The column was washed with 10 column-volumes of equilibration buffer (50 mM Tris-HCl at pH 7.5, 250 mM NaCl, and 10 mM imidazole). The 6 × His-tagged protein was eluted with a 0−250 mM imidazole gradient. The eluted fractions were pooled and added to solid ammonium sulfate (final concentration 1.7 M). The sample was then loaded onto a HiLoad 16/10 phenyl Sepharose column and eluted with a 1.7−0 M decreasing ammonium sulfate gradient. Proteins in the peak fractions were pooled and dialyzed against 50 mM Tris-HCl at pH 7.0. The purity of β-propeller phytase was determined by sodium dodecyl sulfate−polyacrylamide gel electrophoresis (SDS−PAGE) with 4% (w/v) stacking and 12% (w/v) resolving gels. All of the results presented in this study were obtained using this purified 6 × His-tagged phytase.

Inositol Phosphatase Assay. The inositol phosphatase activity of β-propeller phytase was assayed by measuring the rate of increase in inorganic orthophosphate (P_i) using a modified version of the method described by Engelen et al. (*37*). The experiments were conducted in 100 mM Tris-HCl (pH 7.0) under conditions in which the Na−$InsP_6$ concentration (0.01−5.0 mM) and the Ca^{2+} concentration (0−9.0 mM) were varied. To measure activation by Ca^{2+} ions, a Chelex 100 resin (Na form; 200−400 mesh; BioRad) was added to each solution and stirred for 60 min to remove contaminating Ca^{2+} and other metal ions. After filtration, the pH of the solution was checked and readjusted, if necessary, with 0.1 N HCl or 0.1 N NaOH.

The enzymatic reaction was started by the addition of 50 μL of enzyme preincubated with increasing concentrations of Ca^{2+}, followed by the addition of 450 μL of 0.11, 1.1, or 2.2 mM Na−$InsP_6$ that had been preincubated with each of the Ca^{2+} concentrations in 100 mM Tris-HCl (pH 7.0).

The reaction was stopped by adding 500 μL of coloring reagent solution containing 2.5% ammonium heptamolybdate, 0.175% ammonia, 0.1425% ammonium vanadate, and 22.75% nitric acid. The absorbance of the solution was measured at 415 nm.

TLC Analysis of Reaction Products. Cellulose-precoated glass plates (without the fluorescent indicator) were obtained from Merck (Darmstadt, Germany). The plate dimensions were 20 × 20 cm^2, and the coating thickness was 100 mm. The plates were developed in a double-through chamber (internal dimensions: 30 × 27 × 10 cm^3). Then, 2−5 μL of 50 mL total-volume samples were applied at a distance of 1 cm from the plate. A 20-mL volume of the mobile phase consisting of 1-propanol/25% ammonia solution/water (5:

4:1) was used per experiment, and the distance between the upper level of the mobile phase and the lower borders of the application zones was kept as short as possible (*38*). The plates were developed at room temperature until the solvent front was 5−10 mm away from the upper plate border. Running time was approximately 12 h.

The detection of phosphate and InsPs was carried out as follows. The developed cellulose plates were air-dried and sprayed with molybdate reagent containing 8 mM ammonium heptamolybdate tetrahydrate, 0.1 M HCl, and 0.5 M $HClO_4$. The plates were subsequently incubated at 85 °C for 6.5 min and exposed to UV light (254 nm) at a distance of 20 cm for another 6.5 min. Faint blue spots were immediately visible after UV exposure, and the maximal color intensity of the spots was obtained in 2 h. To avoid background formation and fading of the spots, processed plates were kept out of bright light.

Identification of Phytate Hydrolysis Products. The enzymatic reaction was performed in the presence of 2 mM Na−$InsP_6$ in a 100 mM Tris-HCl buffer (pH 7.0) with varying concentrations of Ca^{2+}, in a final volume of 50 mL. The enzymatic reaction was started by the addition of a suitable enzyme solution to the reaction solution at 37 °C. The samples (500 μL) were removed periodically from the reaction mixture, and the total amount of liberated phosphate was quantified by the previously described ammonium molybdate method. After the enzymatic reaction was saturated, aliquots of each sample were applied to a TLC plate with a pipet. The plate was developed at room temperature, and the hydrolysis products were analyzed.

Isolation of Phytate Hydrolysis Products. The reaction mixture (250 mL) for $InsP_6$ hydrolysis contained 100 mM Tris-HCl (pH 7.0), 2 mM Na−$InsP_6$, 2 mM or 0.1 mM $CaCl_2$, and an aliquot of β-propeller phytase in a final volume of 250 mL. After incubation at 37 °C for 24 h, the total amount of phosphates and InsPs were analyzed. Each incubation mixture was lyophilized, and the dry residues were dissolved in 5 mL of distilled water. The solutions were loaded onto a Dowex column (Sigma, 2.0 × 25 cm) equilibrated with distilled water at a flow rate of 3.0 mL/min. The column was washed with 100 mL of 0.1 M HCl. The bound InsPs were eluted with a linear gradient of 0.1−1.0 M HCl at 3.0 mL/min. Even-numbered fractions were checked by TLC analysis. The fraction tubes corresponding to the InsPs were pooled, adjusted to pH 7.0 with 1.0 N NaOH, and lyophilized until only a dry residue remained. The purity of the InsP preparations was determined by TLC analysis, as described above.

NMR Spectroscopy. Spectra were recorded on a Varian UNITY 500 spectrometer. Lyophilized samples (20−40 mg) were dissolved in D_2O (0.75 mL) and adjusted to pH 7.0 with acetic-d_3 acid-d (CD_3CO_2D) (Sigma). All spectra were recorded at 25 °C. The ^1H NMR spectra were obtained at 500 MHz. The ^1H-chemical shifts were referenced to the residual proton absorption of the solvent D_2O (δ 4.67). The acquisition conditions were as follows: spectral windows, 500 MHz; and pulse width, 50−90° tipping angle. A total of 56 scans were collected for each block with a repetition time of 2.1 s. The total recording time for the 2D spectra including ^1H-^1H COSY and HMQC was 17 h.

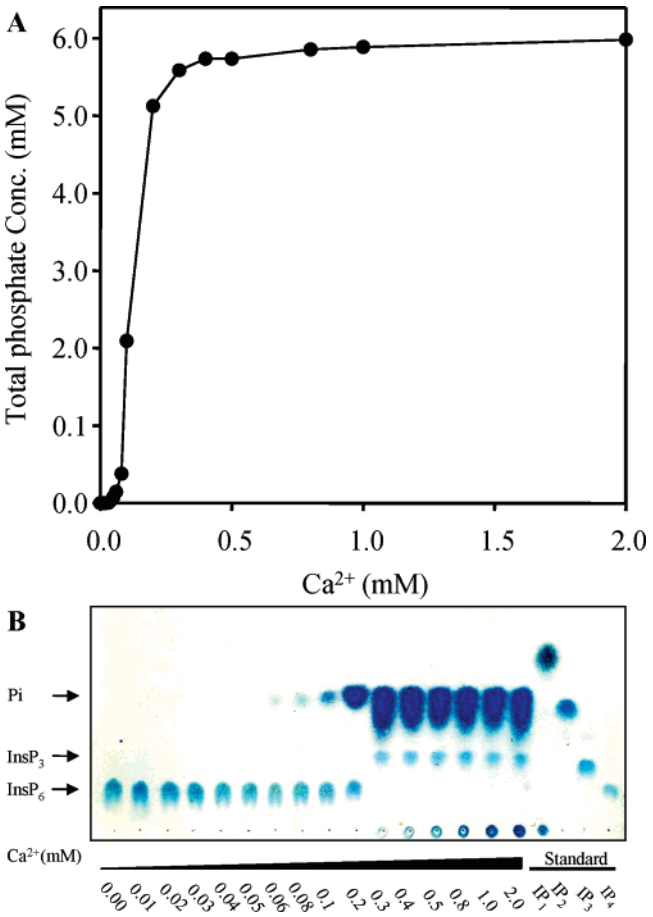

FIGURE 1: Kinetic experiments (A) and TLC analysis (B) show that the β-propeller phytase has substrate specificity for Ca^{2+}−$InsP_6$. To determine the effect of Ca^{2+} on $InsP_6$ hydrolysis, the Ca^{2+} concentration was varied at 2 mM Ca^{2+}-free-$InsP_6$ in 100 mM Tris-HCl (pH 7.0). When the reactions were completed after 20 min, the effect of Ca^{2+} on $InsP_6$ hydrolysis was analyzed by quantifying the total liberated phosphate and TLC analysis of each reaction solution (1 μL). Lanes 1−16 represent the reaction solutions with Ca^{2+} concentrations of 0, 0.01, 0.02, 0.03, 0.04, 0.05, 0.06, 0.08, 0.1, 0.2, 0.3, 0.4, 0.5, 0.8, 1.0, and 2.0 mM, respectively, with 2 mM $InsP_6$; lane 17, Ins2P; lane 18, Ins(5,6)P_2; lane 19, Ins-(1,4,5)P_3; and lane 20, Ins(1,3,4,5)P_4.

RESULTS AND DISCUSSION

The kinetic experiments and TLC analysis show that the β-propeller phytase has substrate specificity for Ca^{2+}−$InsP_6$ and yields an $InsP_3$ and three phosphate groups as the final products. Previous kinetic experiments strongly suggested that β-propeller phytase requires Ca^{2+}, not only as an essential activator but also as a part of its substrate, Ca^{2+}−$InsP_6$. Further kinetic experiments indicated that Na−$InsP_6$ acted as a competitive inhibitor (*26*).

To better understand the kinetic mechanism and the specific role of Ca^{2+} in $InsP_6$ hydrolysis by β-propeller phytase, the following studies were carried out. β-Propeller phytase was preincubated with increasing concentrations of Ca^{2+}, followed by the addition of 2 mM Na−$InsP_6$, which had been preincubated with each concentration of Ca^{2+}. When the reaction was completed after 20 min, each reaction solution was analyzed by quantifying the total amount of liberated phosphate (Figure 1A) or by TLC (Figure 1B). As shown in Figure 1, β-propeller phytase was totally dependent

on the Ca^{2+} concentration and showed no activity in the absence of Ca^{2+}. However, $InsP_6$ hydrolysis and $InsP_3$ production increased with increasing concentrations of Ca^{2+}. The total liberated phosphate from $InsP_6$ hydrolysis was very close to 6 mM, indicating that the enzyme hydrolyzed three phosphate groups per one $InsP_6$ molecule (Figure 1A). In addition, TLC analysis provided several lines of clear evidence indicating that, in the presence of Ca^{2+}, β-propeller phytase hydrolyzed three phosphates per $InsP_6$ molecule, producing an $InsP_3$ as the final product (Figure 1B). The results of these experiments demonstrate that β-propeller phytase is a specific inositol phosphatase in terms of its unique substrate specificity for $InsP_6$ in the presence of Ca^{2+}.

Ca^{2+}−$InsP_6$ hydrolysis is achieved when the concentration of Ca^{2+}−$InsP_6$ is high and the concentrations of free Ca^{2+} and free $InsP_6$ are minimal. To test the relevance of our β-propeller phytase model and the roles of Ca^{2+} in $InsP_6$ hydrolysis, as a part of the kinetic analyses, we performed zero-order enzyme kinetics instead of initial kinetics for 3 h, using a modified London and Steck's approach, wherein the total amounts of liberated phosphate were determined by fixing the total concentration of Ca^{2+} while varying the total $InsP_6$ concentration and vice versa (*39*). Because β-propeller phytase could not hydrolyze $InsP_6$ at lower concentrations of Ca^{2+}, we sought to determine whether direct complex formation between Ca^{2+} and $InsP_6$ was important for enzyme activity. We measured the total amounts of liberated phosphate at a fixed Ca^{2+} concentration (0.1 mM), while increasing Na−$InsP_6$ (Ca^{2+}-free-$InsP_6$) concentrations from 0 to 5 mM. The enzyme efficiently hydrolyzed nearly three phosphate groups of $InsP_6$ at 0.6 mM Na−$InsP_6$ and 0.1 mM Ca^{2+}. However, the enzyme could not fully hydrolyze the phosphate groups at concentrations above 1.0 mM Na−$InsP_6$ because the small amount of Ca^{2+} was not sufficient for Ca^{2+}−$InsP_6$ chelation with excess amounts of Na−$InsP_6$. When the concentration of Ca^{2+} was lower than that of Na−$InsP_6$, excess amounts of Na−$InsP_6$ increased the Ca^{2+}-free-$InsP_6$ concentration. Therefore, Ca^{2+}-free-$InsP_6$ was not an efficient substrate for β-propeller phytase, and it acted as a competitive inhibitor of the enzyme. These data suggest that the chelation of Ca^{2+} by $InsP_6$ is necessary for enzyme activity against the substrate.

Our earlier studies indicated that, in addition to enzyme inhibition by Ca^{2+}-free-$InsP_6$, excess amounts of Ca^{2+} might act as a competitive inhibitor of the enzyme (*26*). Therefore, we measured the total amounts of liberated phosphate at a fixed Ca^{2+}-free-$InsP_6$ concentration (1 mM), while increasing the Ca^{2+} concentration from 0 to 9 mM (Figure 2B). For these experiments, the enzyme reaction was carried out on a shaking incubator to prevent any Ca^{2+}−$InsP_6$ precipitation. The results showed that the enzyme efficiently hydrolyzed three phosphate groups at about 1.0 mM Ca^{2+} and 1mM Na−$InsP_6$. In contrast, the concentrations of Ca^{2+} below 0.1 mM or above 2 mM decreased enzymatic activity because excess amounts of Ca^{2+} exceeded the capacity of the fixed amount of Na−$InsP_6$ to form Ca^{2+}−$InsP_6$ complexes. These finding are consistent with our previous initial velocity kinetics, indicating that an excess amount of free Ca^{2+} eventually acts as a competitive inhibitor of the enzyme (*26*).

The results in Figure 2A and B reveal that Ca^{2+}−$InsP_6$ hydrolysis is reached when Ca^{2+}−$InsP_6$ complex formation is high and the concentrations of free Ca^{2+} and Ca^{2+}-free-$InsP_6$ are minimal, and high concentrations of free Ca^{2+} and Ca^{2+}-free-$InsP_6$ lead to incomplete $InsP_6$ hydrolysis, which competitively inhibits the enzyme.

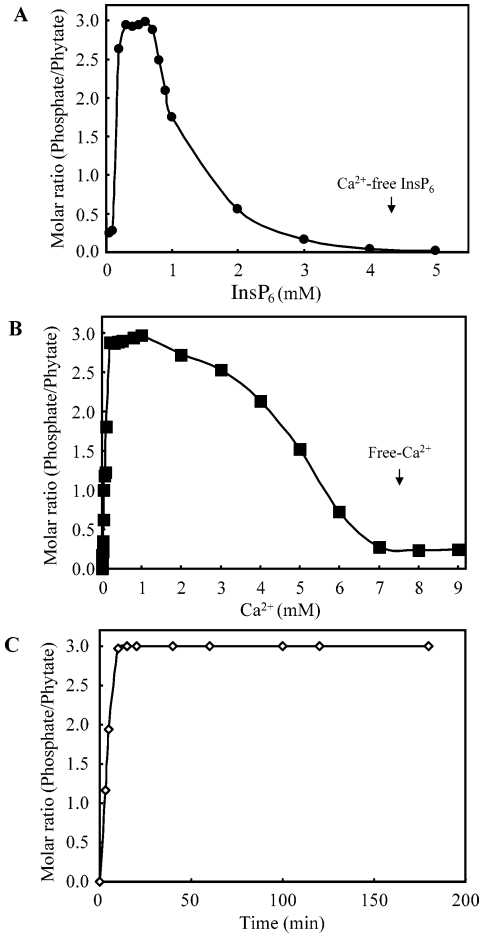

FIGURE 2: Equimolar concentrations of Ca^{2+} and $InsP_6$ are optimal for enzyme reaction. To determine the optimum molar ratio for Ca^{2+}−$InsP_6$ complex formation, the $InsP_6$ concentration was varied at a fixed concentration of 0.1 mM Ca^{2+} (A), and the Ca^{2+} concentration was varied at a fixed concentration of 1.0 mM $InsP_6$ (B). The enzyme reaction was continued for 3 h, and the total liberated phosphate was quantified. (C) Time-course analysis of phosphate hydrolysis using a substrate prepared by mixing 2 mM Ca^{2+} and 2 mM $InsP_6$. The results represent the molar amount of liberated phosphate/mole of $InsP_6$. The maximal enzymatic activity was reached when Ca^{2+}−$InsP_6$ chelation was high, and the concentrations of free Ca^{2+} and Ca^{2+}-free-$InsP_6$ were minimal.

An additional experiment was designed to determine the optimal conditions for Ca^{2+}−$InsP_6$ hydrolysis by the enzyme. We reasoned from the results in Figure 2A and B that equimolar concentrations of Ca^{2+} and $InsP_6$ were optimal for both Ca^{2+}−$InsP_6$ chelation and enzyme reaction. We performed a time-course analysis of the total amount of liberated phosphate using a substrate prepared by mixing equimolar amounts of Ca^{2+} and $InsP_6$. Aliquots of the samples were withdrawn periodically, and the total amounts of liberated phosphate were quantified. The results confirmed that the enzyme efficiently hydrolyzed the substrate at equimolar concentrations of Ca^{2+} and $InsP_6$ within a short period (20 min) and that the enzyme hydrolyzed three phosphate groups from Ca^{2+}−$InsP_6$. Continuing the reaction for an additional 3 h did not hydrolyze any more phosphate groups (Figure 2C).

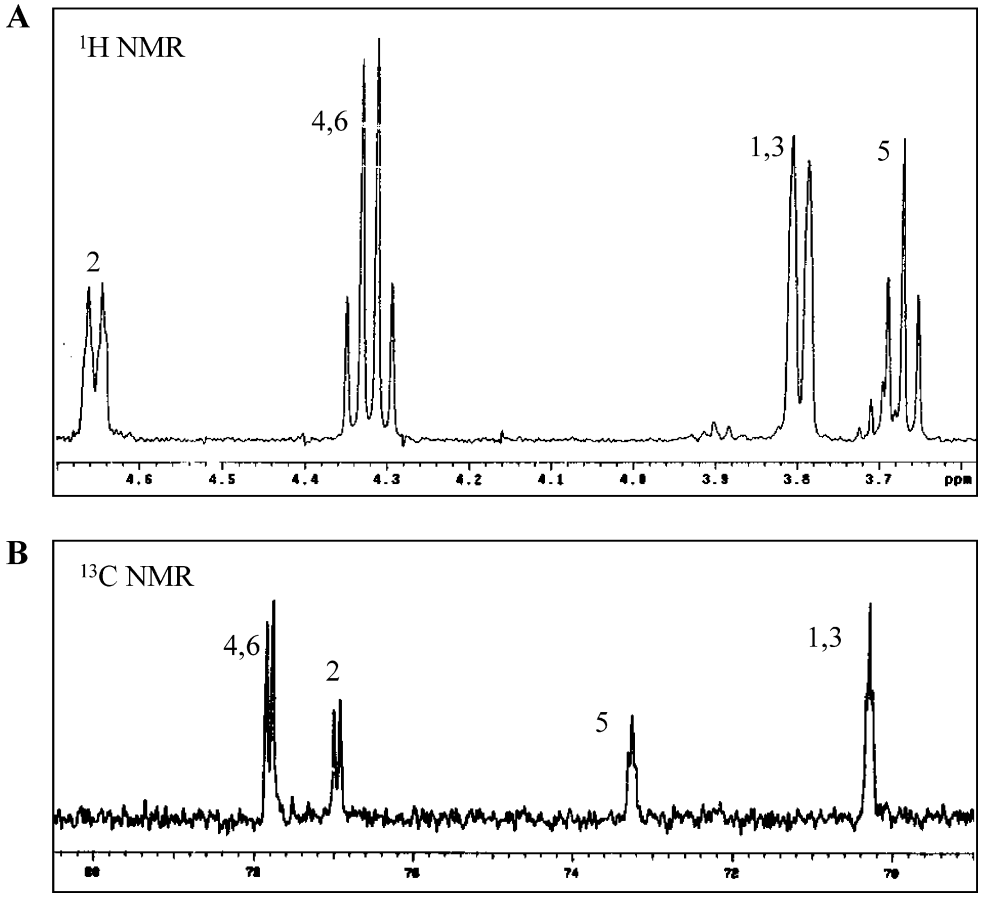

FIGURE 3: (A) ^{1}H- and (B) ^{13}C-NMR spectra of purified *myo*-inositol trisphosphate. *myo*-Inositol trisphosphate was purified by ion-exchange chromatography. The lyophilized sample (22 mg) was dissolved in D_2O (0.75 mL) and adjusted to pH 7.0 with acetic-d_3 acid-*d* (CD_3CO_2D). ^{1}H- and ^{13}C-NMR spectra were recorded on a Varian UNITY 500 spectrometer at 25 °C. The ^{1}H-chemical shifts were referenced to the residual proton absorption of the solvent D_2O (δ 4.67).

From these findings, we assumed that the bidentate (P-Ca^{2+}-P) chelation of Ca^{2+} by two of the six phosphate groups in $InsP_6$ was mandatory for inositol phosphate hydrolysis, thus endowing β-propeller phytase with substrate specificity for $InsP_6$, among several potential phosphate-containing substrates (*40*).

This mechanism is distinct from those of some other enzymes such as HAPs that only hydrolyze Ca^{2+}-free-$InsP_6$ at an acidic pH where Ca^{2+} is dissociated from $InsP_6$ and that show broad substrate specificity for phenyl-phosphate, glucose-1-phosphate, glucose-6-phosphate, and fructose-1-phosphate (*16*).

An NMR analysis of the final product, $InsP_3$, reveals that β-propeller phytase yields myo-inositol-2,4,6-trisphosphate. To understand how β-propeller phytase preferentially recognizes $Ca^{2+}-InsP_6$ and how the enzyme produces an $InsP_3$ from $Ca^{2+}-InsP_6$, we purified the final product, $InsP_3$, using ion-exchange chromatography and TLC analysis and determined the chemical structure of $InsP_3$. Purified $InsP_3$ was analyzed by 1D (^{1}H- and ^{13}C-) and 2D NMR spectroscopy. The ^{1}H NMR spectrum of the purified $InsP_3$ is shown in Figure 3A. The spectrum of $InsP_3$ consisted of four distinct sets of protons in a 1:2:2:1 ratio of, indicating a plane of symmetry in the molecule. This was consistent with observations that equatorial proton resonance was generally downfield of axial protons. The one equatorial proton H-2 at δ 4.64 was split into a triplet of doublets, which appeared as broad doublets because of one large $J_{H(2)-P}$ coupling and two small J_{ax-eq} vicinal couplings to H-1 and H-3. The magnetically equivalent H-4 and H-6 protons at δ 4.31 were split into quartets because of two J_{ax-ax} vicinal couplings with protons on either side or one J_{H-P} coupling, all of similar magnitude. The magnetically equivalent H-1 and H-3 protons at δ 3.78 were split into a triplet of doublets, which appeared as broad doublets because of one large J_{ax-ax} and small J_{ax-eq} vicinal coupling. The H-5 proton at δ 3.66 was split into a triplet because of two large J_{ax-ax} vicinal couplings to H-4 and H-6 protons. Therefore, the spin system had to be an $InsP_3$.

The ^{13}C NMR spectra of $InsP_3$ consisted of four distinct sets of carbons in a 2:1:1:2 ratio. Further confirmation of the phosphorylated positions in $InsP_3$ was provided by ^{1}H-^{1}H COSY spectra and ^{1}H-decoupled HMQC (δ_H 3.37 → C 70.30, δ_H 4.64 → C 76.97, δ_H 4.31 → C 77.82, δ_H 3.66 → C 72.26), which showed $^2J_{C-P}$ and $^3J_{H-P}$ connectivities at C-2, C-4, and C-6 (Figure 3B; Supporting Information Figure 1). From these studies, we determined that the $InsP_3$ was *myo*-Ins(2,4,6)P_3 (Table 1). To determine the pathway of β-propeller phytase-catalyzed $Ca^{2+}-InsP_6$ hydrolysis, we performed the enzyme reaction directly in the D_2O solution, purified the reaction intermediates after partial hydrolysis of $Ca^{2+}-InsP_6$, and further analyzed the chemical structure of the intermediates. The results showed a mixture of *myo*-Ins(2,4,6)P_3 and *myo*-Ins(2,4,5,6)P_4, as summarized in Table 2.

Table 1: ^{1}H- and ^{13}C-NMR Spectral Data for *myo*-Inositol-2,4,6-trisphosphate

positions	$^{\delta}$H	$^{\delta}$C[a]
1,3	3.78 (2H, br. d, $J = 9.5$)[b]	70.30 (t, $^{3}J_{C-P} = 3.03$)[c]
2	4.64 (1H, dt, $^{3}J_{H-P} = 8.5$, $J_{eq-ax} = 1.5-2.0$)	76.97 (d, $^{2}J_{C-P} = 6.00$)
4,6	4.31 (1H, dt, $^{3}J_{H-P} = 9.2$, $J_{ex-ax} = 9.5-9.0$)	77.82 (d, $^{2}J_{C-P} = 6.08$)
5	3.66 (1H, t, $J_{ax-ax} = 9.0$)	73.26 (t, $^{3}J_{C-P} = 3.34$)

[a] Assigned with ^{1}H-decoupled ^{13}C-NMR spectrum. [b] Proton resonance integration, multiplicity, and coupling constants are indicated in parentheses. [c] ^{13}C-resonance multiplicity and coupling constants are indicated in parentheses.

Table 2: ^{1}H- and ^{13}C-NMR Spectral Data for *myo*-Inositol-2,4,5,6-tetraphosphate

positions	$^{\delta}$H	$^{\delta}$C[a]
1,3	3.78 (overlapped with H-1,3 of Ins(2,4,6)P_3)[b]	70.11 (br s)[c]
2	4.63 (overlapped with H-2 of Ins(2,4,6)P_3)	76.89 (d, $^{2}J_{C-P} = 6.00$)
4,6	4.39 (2H, q, $J = 9.6$ Hz)	77.08 (m, overlapped with C-2 of Ins(2,4,6)P_3)
5	4.18 (1H, q, $J = 9.2$ Hz)	77.78 (m, overlapped with C-4,6 of Ins(2,4,6)P_3)

[a] Assigned with ^{1}H-decoupled ^{13}C-NMR spectrum. [b] Proton resonance integration, multiplicity, and coupling constants are indicated in parentheses. [c] ^{13}C-resonance multiplicity and coupling constants are indicated in parentheses.

These NMR studies clearly reveal that β-propeller phytase is a special type of inositol phosphatase that catalyzes the sequential hydrolysis of $Ca^{2+}-InsP_6$ to yield *myo*-Ins(2,4,6)-P_3 and three phosphate groups as the final products.

Recently, Kerovuo and co-workers proposed that β-propeller phytase produced *myo*-Ins(1,3,5)P_3 and *myo*-Ins(2,4,6)-P_3 from $InsP_6$ (*31*). However, the final products, as proposed by Kerovuo et al. and our previous computer model building of substrate binding, cannot be reconciled with our current results in terms of chemical structure and the form of $InsP_3$ (*31, 36*). The computer model building of substrate binding was based on the chemical structure proposed by Kerovuo et al., who identified the chemical structures of reaction intermediates and final products on the basis of HPLC comparisons and total phosphate quantification (*31*). Although we reproduced some of their findings, including the formation of Ins(2,4,5,6)P_4 and Ins(2,4,6)P_3, as also confirmed by Greiner et al. (*41*), we were unable to find Ins-(1,3,5)P_3 as a final product (Tables 1 and 2). In particular, our current results are consistent with the important known catalytic property that classifies phytases as 3- or 6-phytases on the basis of the position of the initial hydrolysis of $InsP_6$. It is also well-known that most phytases are unable to hydrolyze an axial phosphate group at the d-2 position of $InsP_6$. Moreover, the formation of both Ins(1,3,5)P_3 and Ins-(2,4,6)P_3 by a single enzyme would require dual 3- and 6-phytase activities, including the cleavage of an axial phosphate group at the d-2 position of phytate (*15, 16, 41*).

Proposed Substrate-Recognition Mechanism of the β-Propeller Phytase. On the basis of the kinetic studies and the physiochemical characteristics of Ca^{2+} and $InsP_6$, we propose an enzyme−substrate binding scheme in the active site of β-propeller phytase (Figure 4A). Three Ca^{2+} ions directly bind the enzyme's active site, which creates an ideal

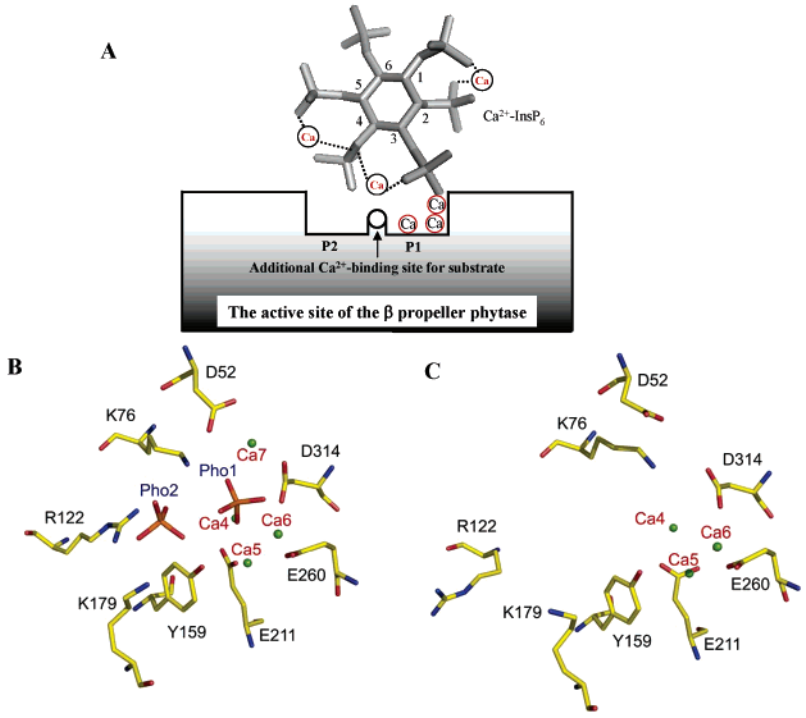

FIGURE 4: Schematic of the proposed $Ca^{2+}-InsP_6$ recognition and binding mechanisms of the β-propeller phytase active site (A) and the active sites of two-phosphate-bound (B) and the phosphate-free (C) structures of β-propeller phytase. We propose this unique substrate-binding mode on the basis of comparative biochemical studies and the final products revealed in this article, although our previous computer-modeling study suggested two alternative binding modes. This was due to the exclusion of an important Ca^{2+} as a $Ca^{2+}-InsP_6$, although the crystal structure of the two-phosphate-bound phytase (pdb accession code: 1QLG) showed an additional Ca^{2+}-binding site compared to that of the phosphate-free phytase (pdb accession code: 1H6L). The crystal structure of an $InsP_6$ molecule bound to an *E. coli* mutant phytase (pdb accession code: 1DKQ) was used (2.05 Å resolution).

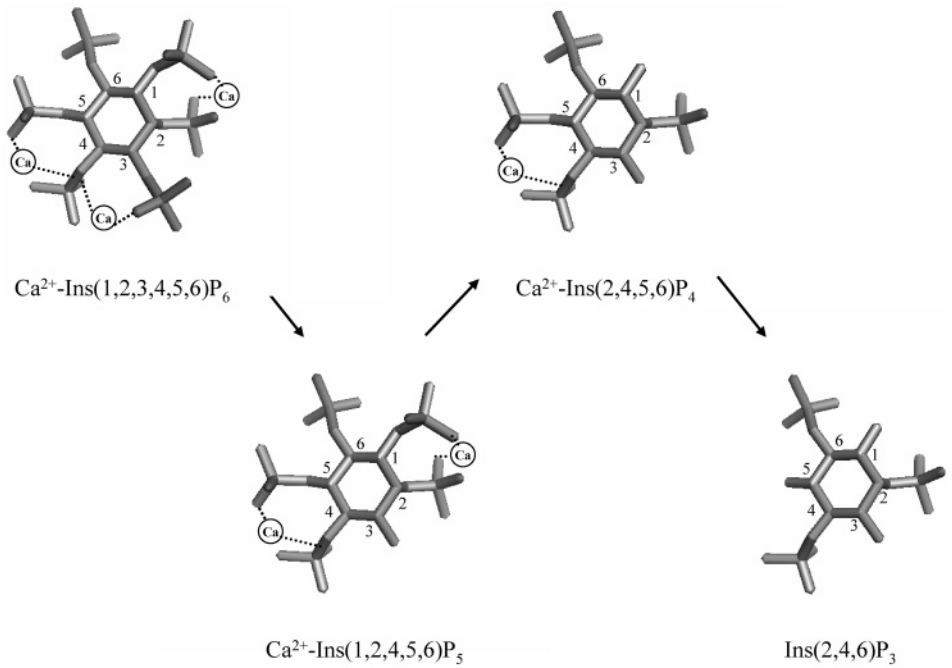

FIGURE 5: Schematic of the proposed hydrolytic pathway of $Ca^{2+}-InsP_6$ catalyzed by β-propeller phytase. The enzyme preferentially recognizes a bidentate (P_3-Ca^{2+}-P_4) of $Ca^{2+}-InsP_6$ as a true substrate and initially hydrolyzes at the d-3 position of Ca^{2+}-phytate. The sequential hydrolysis of two more phosphate groups yields *myo*-Ins(2,4,6)P_3 and three phosphate groups as the final products. It also is possible that the enzyme reaction releases Ca^{2+} ions via dephosphorylation and that the final product, *myo*-Ins(2,4,6)P_3, might lose its Ca^{2+}-binding ability because of the dephosphorylation of adjacent phosphate groups and the long distances (~6.0−6.7 Å) between the remaining phosphate groups. The crystal structure of an $InsP_6$ molecule bound to an *E. coli* mutant phytase (pdb accession code: 1DKQ) was used (2.05 Å resolution).

conformation and charge distribution for $Ca^{2+}-InsP_6$ to fit in. The fourth Ca^{2+} from a bidentate (P-Ca^{2+}-P) of $Ca^{2+}-InsP_6$ binds to one of the enzyme's Ca^{2+}-binding sites in the active site.

This proposal is supported by several lines of evidence. In addition to the biochemical studies in this article, the crystal structure of β-propeller phytase shows important roles for Ca^{2+} in $InsP_6$ hydrolysis. Mg^{2+} cannot stimulate the enzymatic activity, even though Mg^{2+} binding has been shown to overlap with Ca^{2+} binding in the active site of β-propeller phytase (Figure 4B) (*35*). In contrast, among several divalent cations, including Ca^{2+}, Co^{2+}, Fe^{2+}, Mg^{2+}, Mn^{2+}, and Sr^{2+}, only Ca^{2+} and Sr^{2+} stimulate enzymatic activity. Ca^{2+} is ~10-fold more potent than Sr^{2+} in activating the enzyme (*26*). In this regard, similar biochemical and structural results have been reported for Ca^{2+}-channel opening in the Ins(1,4,5)P_3 receptor (IP3R), in that low concentrations of Ca^{2+} and high concentrations of Sr^{2+} were shown to be effective for IP3R Ca^{2+}-channel opening (*42*−*44*). This is consistent with the relative abilities of Ca^{2+} and Sr^{2+} to stimulate β-propeller phytase (*44*).

We reasoned that the ability of Ca^{2+} (0.99 Å) or Sr^{2+} (1.10 Å) to activate enzymatic activity might be due to their larger ionic radii compared to that of Mg^{2+} (0.65 Å) (*45*, *46*). These results could be rationalized by the chelation of Ca^{2+} by InsPs (Scheme 1). In fact, InsPs and $InsP_6$ have much higher affinities for Ca^{2+} than for Mg^{2+}, and these InsPs can form bidentate P-Ca^{2+}-P between Ca^{2+} and two adjacent phosphate groups on the inositol ring (*7*). This idea is supported by our previous isothermal titration calorimetry (ITC) studies, indicating that 4 mol of Ca^{2+} strongly bind to 1 mol of $InsP_6$ with dissociation constants of 0.67, 2.22, 34.60, and 246 μM, respectively (*26*). $InsP_6$ is also known as a strong chelator of Ca^{2+} and, in nature, exists as $Ca^{2+}-InsP_6$ in plant seeds (*47*). Therefore, it is possible that β-propeller phytase may be designated to preferentially recognize $Ca^{2+}-InsP_6$ as its true substrate.

Finally, the crystal structures of β-propeller phytase in two different states provide direct evidence that β-propeller phytase selectively binds $Ca^{2+}-InsP_6$ as a substrate. The crystal structure of β-propeller phytase shows one additional Ca^{2+}-binding site in the two-phosphate-bound structure of its active site (*36*) (Figure 4B) compared with those in the phosphate-free structure (*35*) (Figure 4C). This additional Ca^{2+} might originate from $Ca^{2+}-InsP_6$. These findings strongly support a specific role for $Ca^{2+}-InsP$ chelation in substrate specificity determination. This unique $Ca^{2+}-InsP$ chelation may provide an explanation as to how the enzymes associated with InsPs preferentially recognize their substrate $Ca^{2+}-InsPs$. Therefore, $Ca^{2+}-InsP$ chelation might endow β-propeller phytase with selective substrate specificity.

Proposed β-Propeller Phytase-Catalyzed Pathway of $Ca^{2+}-InsP_6$ Hydrolysis. On the basis of our NMR studies of reaction intermediates and the final product, we propose a sequential hydrolytic pathway of $Ca^{2+}-InsP_6$ catalyzed by β-propeller phytase. This proposal can also explain how the enzyme specifically produces *myo*-Ins(2,4,6)P_3 as a final product from $Ca^{2+}-InsP_6$ (Figure 5).

A bidentate (P_3-Ca^{2+}-P_4) of $Ca^{2+}-InsP_6$ initially binds to two phosphate-binding sites in the active site of β-propeller phytase, which preferentially hydrolyzes the phosphate group at the d-3 position of $Ca^{2+}-InsP_6$ to release Ins(1,2,4,5,6)P_5 as an initial product (*48*). After the hydrolysis of the first phosphate group, the enzyme binds another bidentate (P_1-Ca^{2+}-P_2) of Ins(1,2,4,5,6)P_5, followed by the hydrolysis of the phosphate group at the d-1 position to release Ins(2,4,5,6)-

P_4, as identified by NMR analysis of reaction intermediates (Table 2). Finally, the enzyme binds a bidentate (P_5-Ca^{2+}-P_4) of Ins(2,4,5,6)P_4 and eventually hydrolyzes the phosphate group at the d-5 position to yield *myo*-Ins(2,4,6)P_3 as a final product. Under these experimental conditions, the final product, *myo*-Ins(2,4,6)P_3, is not further hydrolyzed. This result can be explained by the unique characteristics of *myo*-Ins(2,4,6)P_3: the absence of an adjacent phosphate group and the inability of Ca^{2+} to bind to *myo*-Ins(2,4,6)P_3. In addition, this final product cannot mediate a bidentate formation with Ca^{2+} because of the long distances between the phosphate groups (~6.0−6.7 Å; Figure 5).

In physiological conditions, $InsP_6$ is easily complexed with several divalent metal ions, such as Ca^{2+}, Mg^{2+}, Co^{2+}, and Fe^{2+}, because of the strong negative ionic charge of its six phosphate groups. Among these several metal ions, Ca^{2+}−$InsP_6$ is a major complex because Ca^{2+} is the most abundant divalent metal ion in plant seeds (*9*, *42*). Therefore, the catalytic properties of β-propeller phytase may provide another aspect of biotechnological applications, especially for the reduction of antinutritional effects of food with high Ca^{2+}−$InsP_6$ content. Because β-propeller phytase is an extracellular enzyme from *Bacillus amyloliquefacience*, the microorganisms secrete β-propeller phytase into the medium where, in plant seeds under most mild environmental conditions, the Ca^{2+}−$InsP_6$ complex may exist primarily in the pH range of 5.0−8.5. Therefore, β-propeller phytase may have a role in making Ca^{2+}−$InsP_6$ soluble for microorganisms or plants by liberating both Ca^{2+} and phosphate groups from extracelluar Ca^{2+}−$InsP_6$ (*34*, *48*).

Perspective: The Selective Interactions between Ca^{2+} and Inositol Phosphates. Inositol phosphates are present in almost all living cells, both on the inside of the plasma membrane as phosphatidyl inositol phosphates (PtdInsPs) and in various discrete subcellular compartments. Inositol phosphates constitute a family of naturally existing chelators for biologically important Ca^{2+}, which have largely gone unrecognized, not only because of the relatively sophisticated chemical structures of inositol phosphate derivatives but also because of their diverse chelating characteristics for several divalent cations, such as Co^{2+}, Fe^{2+}, Mg^{2+}, and Mn^{2+}. Several inositol phosphates, such as PtdIns(4,5)P_2, Ins(1,4,5)P_3, Ins(1,3,4,5)-P_4, and $InsP_6$, may exist as Ca^{2+}-inositol phosphates because their binding affinities are quite high within the range of Ca^{2+} concentrations found in biological systems (10^{-7}−10^{-3} M) (*7*, *49*). Ins(1,4,5)P_3 and $InsP_6$, with two adjacent phosphate groups, have higher affinity for Ca^{2+} than for Mg^{2+}, primarily due to the difference in their ionic radii (*16*). However, $InsP_1$ or ATP with its three adjacent phosphate groups has stronger affinity for Mg^{2+} than for Ca^{2+}. The phosphate groups in ATP are much closer than those in InsPs, which may be more favorable for Mg^{2+} because of its small ionic radius. This principle is supported by the physiological observations that enzymes requiring ATP are totally dependent on Mg^{2+} because Mg^{2+}-ATP, rather than Ca^{2+}-ATP, is the true substrate (*50*). The results in this article demonstrate that the unique Ca^{2+}−InsPs chelation is highly specific and causes β-propeller phytase to preferentially recognize its specific substrate. Therefore, the kinetic mechanism of β-propeller phytase may provide evidence for the selective chelation of Ca^{2+} by two adjacent phosphates in biological systems.

ACKNOWLEDGMENT

We thank Yong-Hee Lee, Sang-Hyun Lee, Sung-Woo Lee, Sang-Yeon Park, and Steven E. Shoelson of Harvard Medical School for helpful discussions.

SUPPORTING INFORMATION AVAILABLE

Two-dimensional ^{1}H-^{1}H COSY and ^{1}H-decoupled HMQC spectra of myo-inositol triphosphate recorded on a Varian UNITY 500 spectrometer at 25 °C. This material is available free of charge via the Internet at http://pubs.acs.org.

REFERENCES

1. Tanford, C. (1984) The sarcoplasmic reticulum calcium pump. Localization of free energy transfer to discrete steps of the reaction cycle, *FEBS Lett 166*, 1−7.
2. Luttrell, B. M. (1994) Cellular actions of inositol phosphates and other natural calcium and magnesium chelators, *Cell Signal 6*, 355−62.
3. Martin, C. J., and Evans, W. J. (1986) Phytic acid-metal ion interactions. II. The effect of pH on Ca(II) binding, *J. Inorg. Biochem. 27*, 17−30.
4. Vohra, P., Gray, A., and Kratzer, F. H. (1965) Phytic acid-metal complexes, *Proc. Soc. Exp. Biol. Med. 120*, 447−449.
5. Jonson, L. F., and Tate, M. E. (1969) The conformational analysis of phytic acid based on NMR spectra, *J. Chem. 47*, 63−73.
6. Cheryan, M. (1980) Phytic acid interactions in food systems, *Crit. Rev. Food Sci. Nutr. 13*, 297−335.
7. Luttrell, B. M. (1993) The biological relevance of the binding of calcium ions by inositol phosphates, *J. Biol. Chem. 268*, 1521−1524.
8. Sandstrom, B., Cederblad, A., Stenquist, B., and Andersson, H. (1990) Effect of inositol hexaphosphate on retention of zinc and calcium from the human colon, *Eur. J. Clin. Nutr. 44*, 705−708.
9. Marini, M. A., Evans, W. J., and Morris, N. M. (1985) Calorimetric and potentiometric studies on the binding of calcium by phytic acid, *J. Appl. Biochem. 7*, 180−191.
10. Grases, F., Costa-Bauza, A., Perello, J., Isern, B., Vucenik, I., Valiente, M., Munoz, J. A., and Prieto, R. M. (2006) Influence of concomitant food intake on the excretion of orally administered myo-inositol hexaphosphate in humans, *J. Med. Food 9*, 72−76.
11. Grases, F., Sanchis, P., Perello, J., Isern, B., Prieto, R. M., Fernandez-Palomeque, C., Fiol, M., Bonnin, O., and Torres, J. J. (2006) Phytate (myo-inositol hexakisphosphate) inhibits cardiovascular calcifications in rats, *Front Biosci. 11*, 136−142.
12. Malberti, F., and Ravani, P. (2005) Control of calcium and phosphate metabolism and prevention of vascular calcifications in uremic patients, *G. Ital. Nefrol. 31*, S47−S52.
13. Greiner, R., Konietzny, U., and Jany, K. D. (1993) Purification and characterization of two phytases from *Escherichia coli*, *Arch. Biochem. Biophys. 303*, 107−113.
14. Lei, X. G., and Stahl, C. H. (2001) Biotechnological development of effective phytases for mineral nutrition and environmental protection, *Appl. Microbiol. Biotechnol. 57*, 474−481.
15. Mullaney, E. J., and Ullah, A. H. (2003) The term phytase comprises several different classes of enzymes, *Biochem. Biophys. Res. Commun. 312*, 179−184.
16. Oh, B. C., Choi, W. C., Park, S., Kim, Y. O., and Oh, T. K. (2004) Biochemical properties and substrate specificities of alkaline and histidine acid phytases, *Appl. Microbiol. Biotechnol. 63*, 362−372.
17. Wodzinski, R. J., and Ullah, A. H. (1996) Phytase, *Adv. Appl. Microbiol. 42*, 263−302.
18. Van Etten, R. L., Davidson, R., Stevis, P. E., MacArthur, H., and Moore, D. L. (1991) Covalent structure, disulfide bonding, and identification of reactive surface and active site residues of human prostatic acid phosphatase, *J. Biol. Chem. 266*, 2313−2319.
19. Lim, D., Golovan, S., Forsberg, C. W., and Jia, Z. (2000) Crystal structures of *Escherichia coli* phytase and its complex with phytate, *Nat. Struct. Biol. 7*, 108−113.
20. Wyss, M., Brugger, R., Kronenberger, A., Remy, R., Fimbel, R., Oesterhelt, G., Lehmann, M., and van Loon, A. P. (1999) Biochemical characterization of fungal phytases (myo-inositol hexakisphosphate phosphohydrolases): catalytic properties, *Appl. Environ. Microbiol. 65*, 367−373.

21. Barrientos, L., Scott, J. J., and Murthy, P. P. (1994) Specificity of hydrolysis of phytic acid by alkaline phytase from lily pollen, *Plant Physiol. 106*, 1489−1495.
22. Cheng, C., and Lim, B. L. (2006) Beta-propeller phytases in the aquatic environment, *Arch. Microbiol.* 1−13.
23. Kerovuo, J., Lauraeus, M., Nurminen, P., Kalkkinen, N., and Apajalahti, J. (1998) Isolation, characterization, molecular gene cloning, and sequencing of a novel phytase from *Bacillus subtilis*, *Appl. Environ. Microbiol. 64*, 2079−2085.
24. Kerovuo, J., Lappalainen, I., and Reinikainen, T. (2000) The metal dependence of *Bacillus subtilis* phytase, *Biochem. Biophys. Res. Commun. 268*, 365−369.
25. Kim, Y. O., Lee, J. K., Kim, H. K., Yu, J. H., and Oh, T. K. (1998) Cloning of the thermostable phytase gene (phy) from Bacillus sp. DS11 and its overexpression in *Escherichia coli*, *FEMS Microbiol. Lett. 162*, 185−191.
26. Oh, B. C., Chang, B. S., Park, K. H., Ha, N. C., Kim, H. K., Oh, B. H., and Oh, T. K. (2001) Calcium-dependent catalytic activity of a novel phytase from Bacillus amyloliquefaciens DS11, *Biochemistry 40*, 9669−9676.
27. Powar, V. K., and Jagannathan, V. (1982) Purification and properties of phytate-specific phosphatase from *Bacillus subtilis*, *J. Bacteriol. 151*, 1102−1108.
28. Jog, S. P., Garchow, B. G., Mehta, B. D., and Murthy, P. P. (2005) Alkaline phytase from lily pollen: Investigation of biochemical properties, *Arch. Biochem. Biophys. 440*, 133−140.
29. Garchow, B. G., Jog, S. P., Mehta, B. D., Monosso, J. M., and Murthy, P. P. (2005) Alkaline phytase from Lilium longiflorum: Purification and structural characterization, *Protein Expression Purif. 46* (2), 221−232.
30. Tye, A. J., Siu, F. K., Leung, T. Y., and Lim, B. L. (2002) Molecular cloning and the biochemical characterization of two novel phytases from B. subtilis 168 and B. licheniformis, *Appl. Microbiol. Biotechnol. 59*, 190−197.
31. Kerovuo, J., Rouvinen, J., and Hatzack, F. (2000) Analysis of myo-inositol hexakisphosphate hydrolysis by Bacillus phytase: indication of a novel reaction mechanism, *Biochem. J. 352*, 623−628.
32. Hara, A., Ebina, S., Kondo, A., and Funagua, T. (1985) A new type of phytase from Typha latifolia L, *Agric. Biol. Chem. 49*, 3539−3544.
33. Scott, J. J., Loewus, F. A. (1986) A calcium-activated phytase from pollen of *Lilium longiflorum*, *Plant Physiol. 82*, 333−335.
34. Chan, W. L., Lung, S. C., and Lim, B. L. (2005) Properties of beta-propeller phytase expressed in transgenic tobacco, *Protein Expression Purif.*
35. Ha, N. C., Oh, B. C., Shin, S., Kim, H. J., Oh, T. K., Kim, Y. O., Choi, K. Y., and Oh, B. H. (2000) Crystal structures of a novel, thermostable phytase in partially and fully calcium-loaded states, *Nat. Struct. Biol. 7*, 147−153.
36. Shin, S., Ha, N. C., Oh, B. C., Oh, T. K., and Oh, B. H. (2001) Enzyme mechanism and catalytic property of beta propeller phytase, *Structure (London) 9*, 851−858.
37. Engelen, A. J., Heeft, F. C. (1993) Simple and rapid determination of phytase activity, *J. AOAC Int. 77*, 761−764.
38. Hatzack, F., and Rasmussen, S. K. (1999) High-performance thin-layer chromatography method for inositol phosphate analysis, *J. Chromatogr., B 736*, 221−229.
39. London, W. P., and Steck, T. L. (1969) Kinetics of enzyme reactions with interaction between a substrate and a (metal) modifier, *Biochemistry 8*, 1767−1779.
40. Kim, Y. O., Kim, H. K. Bae, K. S., Yu, J. H., and Oh, T. K. (1998) Purification and properties of a thermostable phytase from *Bacillus*. sp DS11, *Enzyme Microb. Technol. 22*, 2−7.
41. Greiner, R., Farouk, A., Alminger, M. L., and Carlsson, N. G. (2002) The pathway of dephosphorylation of myo-inositol hexakisphosphate by phytate-degrading enzymes of different Bacillus spp, *Can. J. Microbiol. 48*, 986−994.
42. Serysheva, II, Bare, D. J., Ludtke, S. J., Kettlun, C. S., Chiu, W., and Mignery, G. A. (2003) Structure of the type 1 inositol 1,4,5-trisphosphate receptor revealed by electron cryomicroscopy, *J. Biol. Chem. 278*, 21319−21322.
43. Hamada, K., Terauchi, A., and Mikoshiba, K. (2003) Three-dimensional rearrangements within inositol 1,4,5-trisphosphate receptor by calcium, *J. Biol. Chem. 278*, 52881−52889.
44. Taylor, C. W., da Fonseca, P. C., and Morris, E. P. (2004) IP(3) receptors: the search for structure, *Trends Biochem. Sci. 29*, 210−219.
45. Christianson, D. W., and Cox, J. D. (1999) Catalysis by metal-activated hydroxide in zinc and manganese metalloenzymes, *Annu. Rev. Biochem. 68*, 33−57.
46. Dobereiner, A., Schmid, A., Ludwig, A., Goebel, W., and Benz, R. (1996) The effects of calcium and other polyvalent cations on channel formation by *Escherichia coli* alpha-hemolysin in red blood cells and lipid bilayer membranes, *Eur. J. Biochem. 240*, 454−460.
47. Widdowson, E. M. (1970) Interrelations of dietary calcium with phytates, phosphates and fats, *Bibl. Nutr. Dieta 15*, 38−47.
48. Idriss, E. E., Makarewicz, O., Farouk, A., Rosner, K., Greiner, R., Bochow, H., Richter, T., and Borriss, R. (2002) Extracellular phytase activity of Bacillus amyloliquefaciens FZB45 contributes to its plant-growth-promoting effect, *Microbiology 148*, 2097−2109.
49. Martell, A. E. (1971) Stability constants of metal-ion complexes, *Proc. Chem. Soc., London*, 651.
50. Segel, I. H. (1975) in *Enzyme Kinetics: Substrate-Activator Complex Is the True Substrate*, pp 242−272, John Wiley & Sons, New York.

BI0603118